

Variation of Computed Tomography-Derived Fractional Flow Reserve Related to Different Vessel Morphology

Farklı Damar Morfolojisine Bağlı Bilgisayarlı Tomografi Kaynaklı Fraksiyonel Akım Rezervi Varyasyonları

ABSTRACT

A total of 1492 outpatients with suspected coronary artery disease and who underwent computed tomography-derived fractional flow reserve analysis were examined. To investigate the effects of vessel morphology such as lumen diameter or volume on computed tomography-derived fractional flow reserve, nearly the same or subthreshold values affecting computed tomography-derived fractional flow reserve hemodynamics vessels were compared. Case 1 and 2 present almost the same vessel length (case 1 vs. case 2; 135.0 mm vs. 133.6 mm), low-attenuation plaque volume (0 mm³ vs. 0 mm³), intermediate-attenuation plaque volume (12.5 mm³ vs. 35.5 mm³), and calcified plaque volume (4.7 mm³ vs. 0 mm³) in the right coronary artery. However, lumen volume (877.8 mm³ vs. 2443.7 mm³) and distal computed tomography-derived fractional flow reserve (0.79 vs. 0.96) were markedly different between the 2 patients. Computed tomography-derived fractional flow reserve depends not only on vessel length or plaque characteristics but also on lumen volume or vessel morphology.

Keywords: FFR, FFRCT, luminal volume, plaque, vessel length

ÖZET

Koroner arter hastalığı şüphesi ile bilgisayarlı tomografi kaynaklı fraksiyonel akım rezervi analizi yapılan toplam 1492 ayakta hasta incelendi. Lümen çapı veya hacmi gibi damar morfolojisinin bilgisayarlı tomografi kaynaklı fraksiyonel akım rezervi üzerindeki etkilerini araştırmak için, bilgisayarlı tomografi kaynaklı fraksiyonel akım rezervi damar hemodinamisini etkileyen hemen hemen aynı veya eşik altı değerler karşılaştırılmıştır. Olgu 1 ve Olgu 2, sağ koroner arterde hemen hemen aynı damar uzunluğuna (135,0 mm'ye karşı 133,6 mm), düşük atenüasyon plak hacmine (0 mm³'e karşı 0 mm³), orta seviye atenüasyon plak hacmine (12,5 mm³'e karşı 35,5 mm³) ve kalsifiye plak hacmine (4,7 mm³'e karşı 0 mm³) sahipti. Ancak iki olgu arasında lümen hacmi (877,8 mm³'e karşı 2443,7 mm³) ve distal bilgisayarlı tomografi kaynaklı fraksiyonel akım rezervi (0,79'a karşı 0,96) arasında belirgin şekilde fark vardı. Bilgisayarlı tomografi kaynaklı fraksiyonel akım rezervi, yalnızca damar uzunluğuna veya plak özelliklerine değil, aynı zamanda lümen hacmine veya damar morfolojisine de bağlıdır.

Anahtar Kelimeler: FFR, FFRCT, lümen hacmi, plak, damar uzunluğu

Fractional flow reserve derived from coronary computed tomography (FFR_{CT}) decline from the proximal to the distal segment depending on vessel length¹ or plaque characteristics.¹⁻³ It has been empirically proved that the degree of FFR_{CT} decline varies based on vessel morphology even with constant vessel length. Computed tomography-derived fractional flow reserve and luminal cross-sectional area are closely related³ and tapering of the vessel may contribute to the physiological decline of FFR_{CT}.⁴ However, the effect of lumen volume or vessel morphology on FFR_{CT} remains to be clarified. We present 2 patients with different distal FFR_{CT} changes even though vessel length and plaque characteristics were almost the same for the right coronary artery. The only difference between the 2 patients was lumen volume and vessel morphology (tapered or not tapered).

Case Reports

In these 2 cases, CT angiography (CTA) and invasive coronary angiography did not reveal a significant stenosis in the right coronary artery (RCA). According to the Society

CASE REPORT OLGU SUNUMU

Toshimitsu Tsugu¹ 

Kaoru Tanaka¹ 

Yuji Nagatomo² 

Michel De Maeseneer¹ 

Johan De Mey¹ 

¹Department of Radiology, Universitair Ziekenhuis Brussel, Brussels, Belgium

²Department of Cardiology, National Defense Medical College Hospital, Tokorozawa, Japan

Corresponding author:

Toshimitsu Tsugu
✉ ttsugu@uzbrussel.be

Received: August 18, 2022

Accepted: February 1, 2023

Cite this article as: Tsugu T, Tanaka K, Nagatomo Y, De Maeseneer M, De Mey J. Variation of computed tomography-derived fractional flow reserve related to different vessel morphology. *Turk Kardiyol Dern Ars.* 2023;51(6):419-423.

DOI:10.5543/tkda.2023.60930



Available online at archivestsc.com.
Content of this journal is licensed under a
Creative Commons Attribution -
NonCommercial-NoDerivatives 4.0
International License.

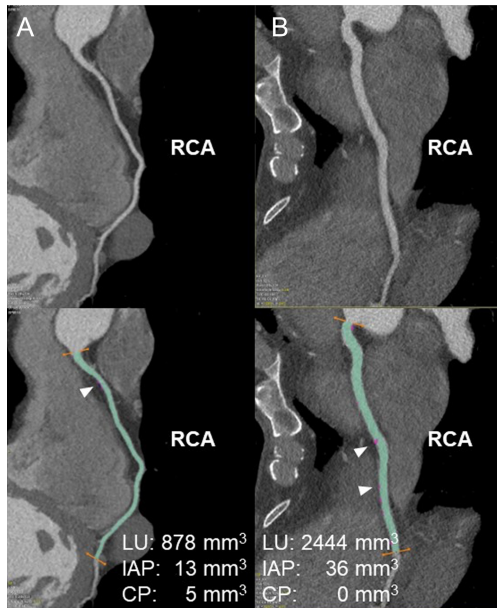


Figure 1. (A) Case 1: CTA showing no significant coronary artery stenosis in the RCA (upper panel). Vessel components are indicated in the following colors: green is LU and red is IAP. The volume of LU, LAP, IAP, and CP are 877.8 mm³, 0 mm³, 12.5 mm³, and 4.7 mm³ (middle panel). The vessel length, ostium, and distal lumen diameter coinciding with FFR_{CT} region of interest are 135.0 mm, 5.8 mm, and 2.9 mm, respectively (lower panel). (B) Case 2: CTA showing no significant coronary artery stenosis in the RCA (upper panel). The volume of LU, LAP, IAP, and CP are 2443.7 mm³, 0 mm³, 35.5 mm³, and 0 mm³ (upper panel). The vessel length is 133.6 mm, 5.8 mm, and 3.8 mm, respectively (lower panel). Arrowhead indicates IAP. CP, calcified plaque; CTA, computed tomography angiography; IAP, intermediate-attenuation plaque; LAP, low-attenuation plaque; LU, lumen; RCA, right coronary artery.

of Cardiovascular Computed Tomography guidelines,⁵ sublingual nitrates (2 sprays of 0.8 mg) were administered 5 minutes before scanning. Computed tomography-derived fractional flow reserve was analyzed by HeartFlow Inc. (Redwood City, Calif., USA). Computed tomography-derived fractional flow reserve was based on the application of computational fluid dynamics to images from CTA. These values are displayed only by specifying any arbitrary point in the coronary artery. The FFR_{CT} was measured at any vessel site from the RCA ostium to the bifurcation of the right posterior descending branch and atrioventricular node. Vessel length, lumen volume, and composition of each vessel were measured using GE AW server 3.2 software (GE Healthcare, Chicago, Ill, USA). Plaque characterization and vessel morphology measurements were performed semi-automatically with Color Code Plaque (GE Healthcare). Vessel constituents were characterized based on Hounsfield units into low-attenuation plaque (LAP) (<30 HU), intermediate-attenuation plaque (IAP) (30-150 HU), and calcified plaque (CP) (>150 HU).¹ Plaque burden was defined as $(1 - \text{lumen area}/\text{outer area}) \times 100\%$ ⁶ The average plaque burden was calculated as the ratio of total plaque volume to vessel volume.⁷ Left ventricular (LV) mass was

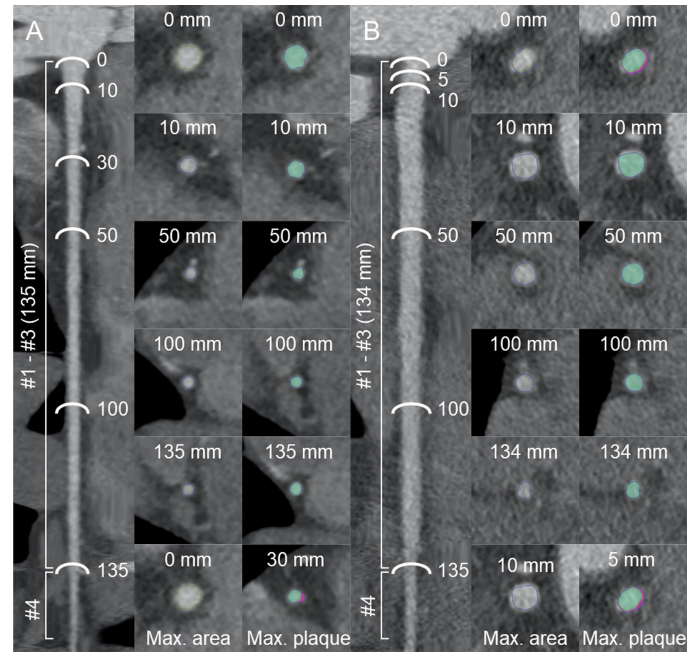


Figure 2. Lumen cross-sectional morphology at each point from the ostium of the right coronary artery. (A) Case 1: Maximal cross-sectional area is 22.7 mm² at 0 mm from the ostium of the RCM. (B) Case 2: Maximal cross-sectional area is 26.4 mm² at 10 mm from the ostium of the RCM. RCA, right coronary artery.

measured using GE AW server 3.2 software (GE Healthcare). The volume of the myocardium extracted from the image data was multiplied by an average value of myocardial tissue density (1.05 g/mL) to calculate LV myocardial mass. Left ventricular mass index was calculated by dividing the LV mass by the body surface area.⁸

Case 1

A 62-year-old woman was admitted with chest discomfort. She had no cardiovascular risk factors (hypertension, diabetes mellitus, dyslipidemia, or smoking). Computed tomography angiography images acquired conditions were heart rate of 56 bpm, CT value of 457 HU, and cardiac cycle of 76% (mid-diastolic phase). Computed tomography angiography did not reveal significant stenosis in the RCA. Vessel length, vessel volume, and lumen volume were 135.0 mm, 895 mm³, and 877.8 mm³, respectively. Low-attenuation plaque, IAP, and CP volume were 0 mm³, 12.5 mm³, and 4.7 mm³, respectively (Figure 1A). Maximal and minimum luminal cross-sectional area were 22.7 mm² (0 mm from the ostium) and 5.1 mm² (135 mm from the ostium) (Figure 2A). Maximum and average plaque burden was 19.5% and 1.9% (Supplementary Table 1). Three-dimensional volume-rendered image of the coronary tree showed no significant vessel tortuosity at the RCA (Figure 3A). Left ventricular mass and LV mass index were 87.0 g and 58.5 g/m² (Figure 4A). Computed tomography-derived fractional flow reserve at the RCA ostium was 1.00 and decreased to 0.79 just proximal to the bifurcation of the right posterior descending branch and atrioventricular node (Figure 5A). Invasive coronary angiography showed no significant stenosis in the RCA (Figure 6A).

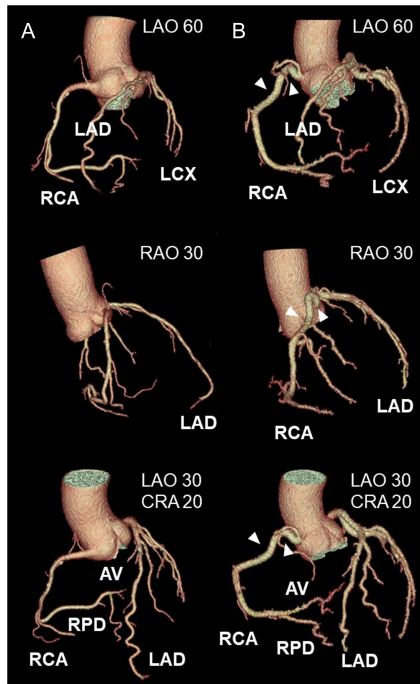


Figure 3. Three-dimensional volume-rendered image of the coronary tree. Upper panel: straight LAO 60 position. Middle panel: straight RAO 30 position. Lower panel: LAO 30 and cranial 20 position. (A) Case 1: No significant vessel tortuosity at the proximal RCA. (B) Case 2: Slight vessel tortuosity (arrowhead) at the distal RCA. AV, atrioventricular node; CRA, cranial; LAD, left anterior descending; LAO, left anterior oblique; LCX, left circumflex; RAO, right anterior oblique; RPD, right posterior descending branch; RCA, right coronary artery; RV, right ventricular branch.

Case 2

A 52-year-old man was admitted because of chest discomfort. He had no cardiovascular risk factors (hypertension, diabetes mellitus, dyslipidemia, or smoking). Computed tomography angiography images acquired conditions were heart rate of 56 bpm, CT value of 465 HU, and cardiac cycle of 77% (mid-diastolic phase). Computed tomography angiography did not reveal a significant stenosis in the RCA. Vessel length, vessel volume, and lumen volume were 133.6 mm, 2479.2 mm³, and 2443.7 mm³, respectively. Low-attenuation plaque, IAP, and CP volume were 0 mm³, 35.5 mm³, and 0 mm³, respectively (Figure 1B). Maximal and minimum luminal cross-sectional area were 26.4 mm² (10 mm from the ostium) and 10.0 mm² (134 mm from the ostium) (Figure 2B). Maximum and average plaque burden were 6.2% and 1.4% (Supplementary Table 1). Three-dimensional volume-rendered image of the coronary tree showed slight vessel tortuosity (arrowhead) at the proximal RCA (Figure 3B). Left ventricular mass and LV mass index were 166.8 g and 89.5 g/m² (Figure 4B). Computed tomography-derived fractional flow reserve at the RCA ostium was 1.00 and gradually decreased to 0.96 just proximal to the bifurcation of the right posterior descending branch and atrioventricular node (Figure 5B). Invasive coronary angiography showed no significant stenosis in the RCA (Figure 6B).

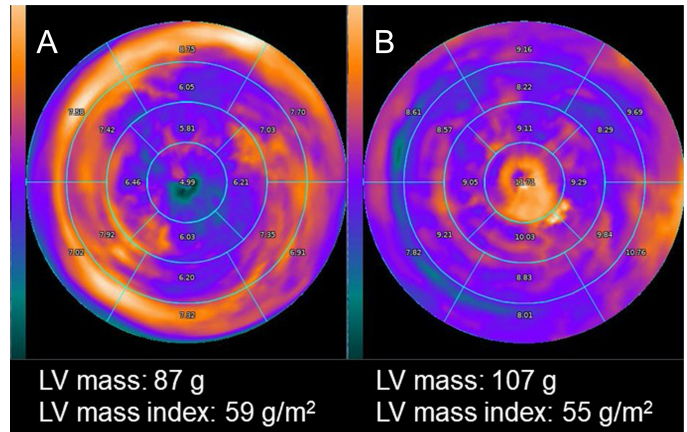


Figure 4. LV mass and LV mass index. (A) Case 1: LV mass 87 g, LV mass index 59 g/m². (B) Case 2: LV mass 107 g, LV mass index 55 g/m². LV, left ventricular.

DISCUSSION

A total of 1492 outpatients with suspected coronary artery disease and who had FFR_{CT} analysis were examined at Universitair Ziekenhuis Brussel between January 2017 and May 2022. To investigate the effects of lumen volume and vessel morphology on FFR_{CT}, 2 cases with almost the same vessel length and similar low plaque volume and burden were compared.

The physiological and progressive decline of FFR_{CT} is related to a variety of factors including vessel length,¹ plaque volume,^{1,2,9} left ventricular mass,⁸ bifurcation angle,¹⁰⁻¹² ramus artery,¹³ and collateral circulation.¹⁴ Previous studies which examined FFR_{CT} in normal coronary arteries showed that FFR_{CT} changes from the

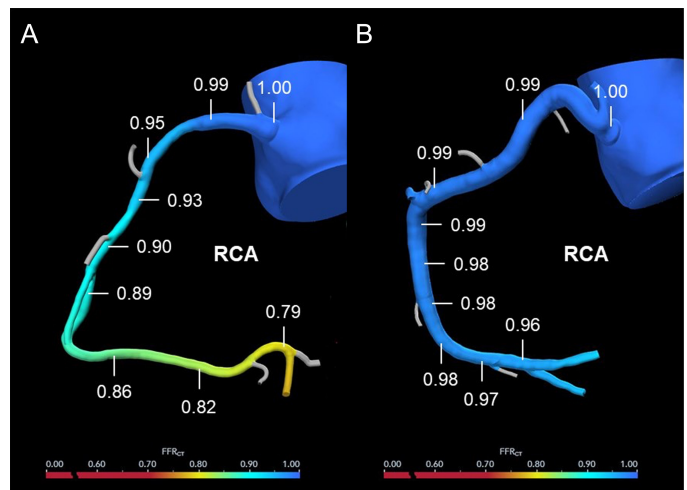


Figure 5. Computed tomography angiography-derived fractional flow reserve. (A) Case 1: FFR_{CT} is 1.00 at the RCA ostium and decreases to 0.79 at just proximal site of the bifurcation of the right posterior descending branch and atrioventricular node. (B) Case 2: FFR_{CT} is 1.00 at the RCA ostium and decreases to 0.96 at just proximal site of the bifurcation of the right posterior descending branch and atrioventricular node. RCA, right coronary artery.

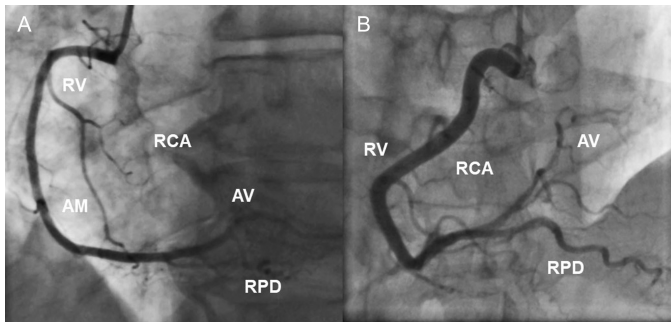


Figure 6. Invasive coronary angiography. (A) Case 1: No significant coronary artery stenosis in the RCA. (B) Case 2: No significant coronary artery stenosis in the RCA. AM, acute marginal branch; AV, atrioventricular node; RPD, right posterior descending branch; RCA, right coronary artery; RV, right ventricular branch.

proximal to the distal segments were smaller in the RCA than that in the left anterior descending (LAD) artery or the left circumflex (LCX) artery.¹ This phenomenon may be related to energy loss due to turbulence caused by the bifurcation angle from the left main trunk (LMT) to LAD or LCX. In the present cases, the RCA was included to avoid the branching influence (from LMT to LAD/LCX or LAD/LCX branches) on FFR_{CT}. Moreover, to avoid the influence of the right posterior descending branch and atrioventricular node, which are major branches in the RCA, vessels from the RCA ostium to just before these branches were compared. The present cases showed different FFR_{CT} changes, lumen volume, and vessel morphology but almost the same vessel length and similar low plaque volume and burden. Several studies have reported a significant association of FFR_{CT} with plaque volume.^{1,9} Deposition of plaque components could lead to impaired functional vasodilatory capacity due to oxidative stress and inflammation, affecting FFR_{CT} hemodynamics.^{15,16} The possibility remained that different plaque characteristics might cause unexpected FFR_{CT} values. Gaur et al² reported that low density non-CP volume of ≥ 30 mm³ predicted FFR_{CT} ≤ 0.80 . In our previous study, the IAP cut-off value for defining FFR_{CT} ≤ 0.80 was 44.8 mm³.¹ The present cases showed that the IAP volume was as small as 13 mm³ and 36 mm³ in case 1 and case 2, respectively. Plaque volume in our cases was smaller than the previously reported thresholds for false positive FFR_{CT}, implicating that the effect on FFR_{CT} could be negligible. Plaque volume and burden were not significant factors that influenced FFR_{CT}, suggesting that luminal morphological differences between cases 1 and 2 played a major role in FFR_{CT} hemodynamics.

Several studies have reported on the effects of vessel morphology on FFR_{CT} from 2 perspectives: luminal cross-sectional area (2D) and vessel volume (3D). At the 2D level (luminal cross-sectional area), Collet et al³ evaluated the variations in FFR_{CT}, luminal cross-sectional area, and plaque area at baseline and after 54 months of follow-up in patients with early-stage of coronary artery disease. Luminal cross-sectional area was correlated with changes in FFR_{CT}, but not plaque area. This study did not examine plaque characteristics (LAP, IAP, and CP), plaque volume, or plaque burden, but it was possible that the plaque volume or plaque burden was low because patients with early

stage of atherosclerosis were enrolled. Computed tomography-derived fractional flow reserve was validated to be significantly correlated with the luminal cross-sectional area at the 2D level. At the 3D level (lumen volume), Holmes et al¹⁷ reported that RCA lumen volume was increased from 1065.8 ± 444.4 to 1147.0 ± 477.8 mm³ by increasing the dose of nitroglycerin. This has a significant effect on coronary vasodilatation and increased FFR_{CT} at distal vessel segments (from 0.91 ± 0.04 to 0.92 ± 0.04). Furthermore, Gassenmaier et al⁴ reported that morphological vessel changes such as tapering may contribute to a physiological FFR_{CT} decline. Hence, a physiological FFR_{CT} decline may be related to vessel morphology. According to Hagen-Poiseuille flow, pressure loss is proportional to the length and inversely proportional to the radius of the lumen diameter. This may explain why FFR_{CT} changes not only depend on vessel length but also on lumen volume.

This case report had some limitations. First, different degrees of vessel tortuosity were observed between cases 1 and 2. Fluid dynamically, a large vessel tortuosity may cause turbulent eddies and energy loss, resulting in FFR_{CT} decline, although there has been no evidence of vessel tortuosity affecting FFR_{CT}. Three-dimensional volume-rendered image of the coronary tree showed that vessel tortuosity was greater in case 2 than in case 1 (Figure 2). However, FFR_{CT} decline was smaller in case 2. A quantitative analysis of turbulent eddies may reveal the effects of different degrees of vessel tortuosity on FFR_{CT} in cases 1 and 2. Our CT equipment could not quantify turbulent eddies. Second, LV mass differed between cases 1 and 2. It was reported that LV myocardial-related parameters (LV mass, LV mass index, LV wall thickness) affected FFR_{CT}. Of LV myocardial-related parameters, LV mass index was the strongest predictor of distal vessel FFR_{CT} > 0.80 and an optimal cut-off value of 66.5 g/m².¹ Left ventricle mass index in both cases 1 and 2 were smaller than the previously reported threshold affecting FFR_{CT} hemodynamics. However, the possibility remained that different LV myocardial-related parameters might cause unexpected FFR_{CT}. Moreover, increased LV mass might cause coronary microvascular dysfunction (CMD), resulting in increased FFR_{CT}. Coronary microvascular dysfunction can be categorized into 3 categories: structural, functional, and extravascular. In the present cases, structural and extravascular abnormalities might be involved in CMD. Luminal obstruction associated with increased LV mass might cause CMD.¹⁸ Coronary microvascular dysfunction requires consideration of myocardial resistance during maximal hyperemia due to impaired endothelial function.¹⁹ Taken together, high microvascular resistance and restricted coronary blood flow caused pressure decrease during maximal hyperemia to be lower than normally expected, resulting in higher FFR_{CT}.

To the best of our knowledge, this is the first report where different distal FFR_{CT} changes were present even though almost the same vessel length and plaque volume was below the previously reported thresholds affecting FFR_{CT}.¹ The main difference between the 2 patients was the lumen volume and vascular morphology (tapered or not tapered). The present cases highlight that FFR_{CT} hemodynamics may affect not only vessel length or plaque volume but also lumen volume or vessel morphology.

Conclusion

Irrespective of the same vessel length, variations in lumen volume or vascular morphology (tapered or not tapered) may contribute to the differences in FFR_{CT} changes.

Informed Consent: Written informed consent was obtained from the patients for the publication of the case report and the accompanying images.

Authorship Contributions: Conception – T.T.; Design – T.T.; Supervision – K.T., Y.N., M.D.M., J.D.M.; Data collection – T.T.; Writing – T.T.; Y.N.; Critical Review – T.T., K.T.

Declaration of Interests: The authors declare that they have no competing interest.

Funding: The authors declare that this study had received no financial support.

References

1. Tsugu T, Tanaka K, Belsack D, et al. Impact of vascular morphology and plaque characteristics on computed tomography derived fractional flow reserve in early stage coronary artery disease. *Int J Cardiol.* 2021;343:187-193. [\[CrossRef\]](#)
2. Gaur S, Øvrehus KA, Dey D, et al. Coronary plaque quantification and fractional flow reserve by coronary computed tomography angiography identify ischaemia-causing lesions. *Eur Heart J.* 2016; 37(15):1220-1227. [\[CrossRef\]](#)
3. Collet C, Katagiri Y, Miyazaki Y, et al. Impact of coronary remodeling on fractional flow reserve. *Circulation.* 2018;137(7):747-749. [\[CrossRef\]](#)
4. Gassenmaier S, Tsiflikas I, Greulich S, et al. Prevalence of pathological FFRCT values without coronary artery stenosis in an asymptomatic marathon runner cohort. *Eur Radiol.* 2021;31(12):8975-8982. [\[CrossRef\]](#)
5. Abbara S, Blanke P, Maroules CD, et al. SCCT guidelines for the performance and acquisition of coronary computed tomographic angiography: A report of the society of cardiovascular Computed Tomography Guidelines Committee: endorsed by the North American Society for Cardiovascular Imaging (NASCI). *J Cardiovasc Comput Tomogr.* 2016;10(6):435-449. [\[CrossRef\]](#)
6. Shi Z, Zhu C, Degnan AJ, et al. Identification of high-risk plaque features in intracranial atherosclerosis: initial experience using a radiomic approach. *Eur Radiol.* 2018;28(9):3912-3921. [\[CrossRef\]](#)
7. Joshi PH, Rinehart S, Vazquez G, et al. A peripheral blood gene expression score is associated with plaque volume and phenotype by intravascular ultrasound with radiofrequency backscatter analysis: results from the ATLANTA study. *Cardiovasc Diagn Ther.* 2013;3(1):5-14. [\[CrossRef\]](#)
8. Tsugu T, Tanaka K, Belsack D, et al. Effects of left ventricular mass on computed tomography derived fractional flow reserve in significant obstructive coronary artery disease. *Int J Cardiol.* 2022;355:59-64. [\[CrossRef\]](#)
9. Ahmadi A, Leipsic J, Øvrehus KA, et al. Lesion-specific and vessel-related determinants of fractional flow reserve beyond coronary artery stenosis. *JACC Cardiovasc Imaging.* 2018;11(4):521-530. [\[CrossRef\]](#)
10. Tsugu T, Tanaka K, Nagatomo Y, Belsack D, De Maeseneer M, De Mey J. Paradoxical changes of coronary computed tomography derived fractional flow reserve. *Echocardiography.* 2022;39(2):398-403. [\[CrossRef\]](#)
11. Tsugu T, Tanaka K. Differences in fractional flow reserve derived from coronary computed tomography angiography according to coronary artery bifurcation angle. *Turk Kardiyol Dern Ars.* 2022;50(1):83-84. [\[CrossRef\]](#)
12. Tsugu T, Tanaka K, Nagatomo Y, et al. Impact of coronary bifurcation angle on computed tomography derived fractional flow reserve in coronary vessels with no apparent coronary artery disease. *Eur Radiol.* 2023;33(2):1277-1285. [\[CrossRef\]](#)
13. Tsugu T, Tanaka K, Nagatomo Y, et al. Impact of ramus coronary artery on computed tomography derived fractional flow reserve (FFRCT) in no apparent coronary artery disease. *Echocardiography.* 2023;40(2):103-112. [\[CrossRef\]](#)
14. Tsugu T, Tanaka K, Belsack D, Jean-François A, Mey J. Impact of collateral circulation with fractional flow reserve derived from coronary computed tomography angiography. *Turk Kardiyol Dern Ars.* 2021;49(8):694-695. [\[CrossRef\]](#)
15. Ahmadi A, Stone GW, Leipsic J, et al. Association of coronary stenosis and plaque morphology with fractional flow reserve and outcomes. *JAMA Cardiol.* 2016;1(3):350-357. [\[CrossRef\]](#)
16. Lavi S, Yang EH, Prasad A, et al. The interaction between coronary endothelial dysfunction, local oxidative stress, and endogenous nitric oxide in humans. *Hypertension.* 2008;51(1):127-133. [\[CrossRef\]](#)
17. Holmes KR, Fonte TA, Weir-McCall J, et al. Impact of sublingual nitroglycerin dosage on FFRCT assessment and coronary luminal volume-to-myocardial mass ratio. *Eur Radiol.* 2019;29(12):6829-6836. [\[CrossRef\]](#)
18. Camici PG, Crea F. Coronary microvascular dysfunction. *N Engl J Med.* 2007;356(8):830-840. [\[CrossRef\]](#)
19. Bartunek J, Sys SU, Heyndrickx GR, Pijls NH, De Bruyne B. Quantitative coronary angiography in predicting functional significance of stenoses in an unselected patient cohort. *J Am Coll Cardiol.* 1995;26(2):328-334. [\[CrossRef\]](#)

Supplementary Table 1. Supplementary Vessel Morphology and Plaque Components

	Case 1	Case 2
Vessel length (mm)	135.0	133.6
Vessel volume (mm ³)	895.0	2479.2
Lumen volume (mm ³)	877.8	2443.7
Low-attenuation plaque volume (mm ³)	0	0
Intermediate-attenuation plaque volume (mm ³)	12.5	35.5
Calcified plaque volume (mm ³)	4.7	0
Maximal plaque burden (%)	19.5	6.2
Average plaque burden (%)	1.9	1.4
Lumen diameter at 0 mm (mm)	5.4	5.1
Lumen diameter at 10 mm (mm)	3.8	5.8
Lumen diameter at 50 mm (mm)	2.8	5.0
Lumen diameter at 100 mm (mm)	2.6	4.1
Lumen diameter at 135 or 134 mm (mm)	2.5	3.6
Lumen cross-sectional area at 0 mm (mm ²)	22.7	20.1
Lumen cross-sectional area at 10 mm (mm ²)	11.2	26.4
Lumen cross-sectional area at 50 mm (mm ²)	6.3	19.4
Lumen cross-sectional area at 100 mm (mm ²)	5.3	13.0
Lumen cross-sectional area at 135 or 134 (mm ²)	5.1	10.0